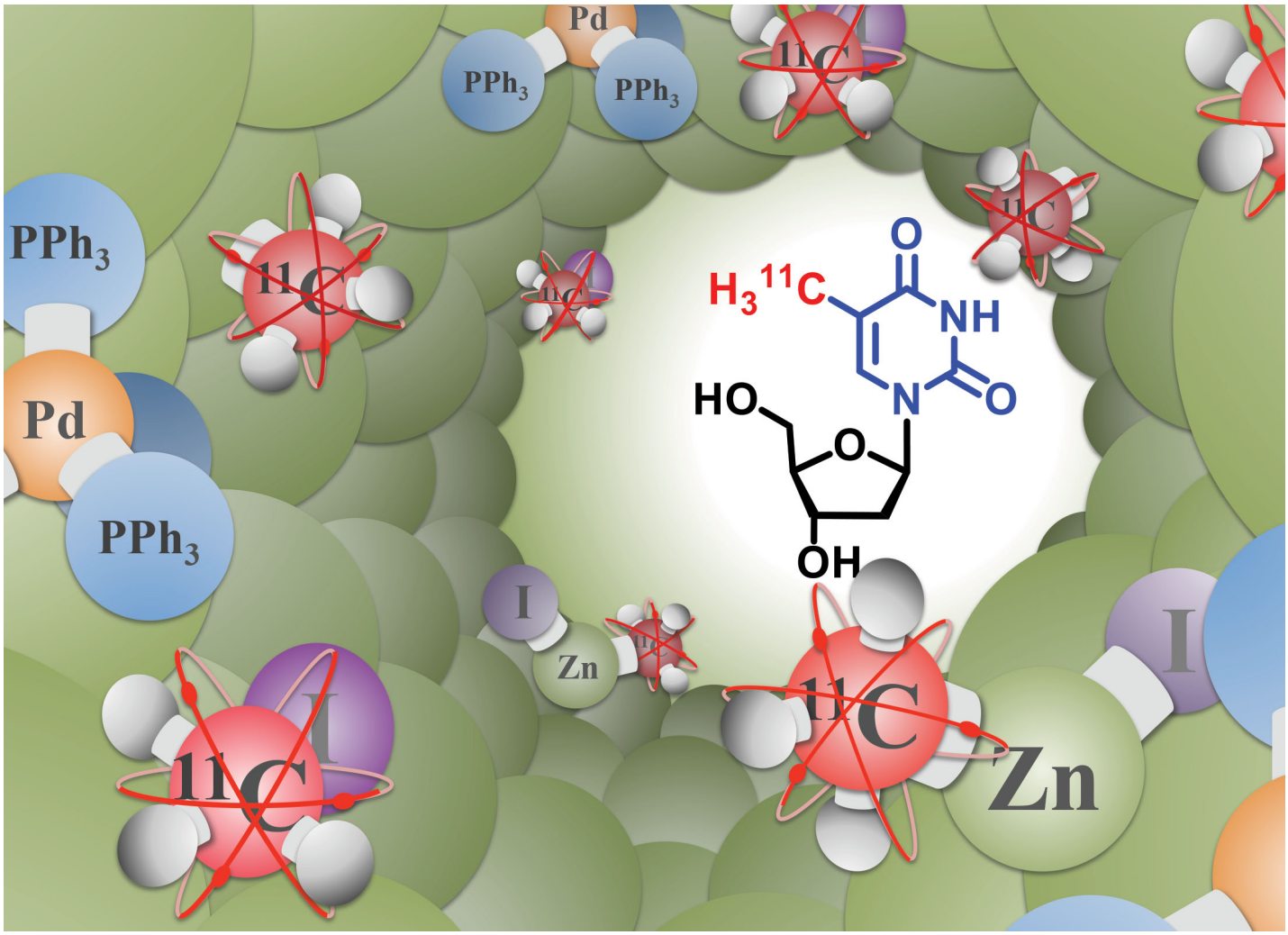

Showcasing research from Dr Jordi Llop's laboratory at CIC biomaGUNE, San Sebastian, Spain.

Negishi coupling reactions with [^{11}C]CH_3I: a versatile method for efficient ^{11}C–C bond formation

An easy, fast and efficient one-pot method allows for ^{11}C–C bond formation *via in situ* production of [^{11}C]CH_3ZnI, affording a wide range of functionalized [^{11}C]methyl aryls, including [^{11}C] thymidine, thus changing the way ^{11}C-radiolabelling could be performed in the future.

As featured in:

See Luka Rejc, Jordi Llop *et al.*, *Chem. Commun.*, 2018, **54**, 4398.

ROYAL SOCIETY OF CHEMISTRY

rsc.li/chemcomm

Registered charity number: 207890

ChemComm

COMMUNICATION

View Article Online
View Journal | View Issue

Check for updates

Cite this: *Chem. Commun.*, 2018, **54**, 4398

Received 24th February 2018,
Accepted 26th March 2018

DOI: 10.1039/c8cc01540f

rsc.li/chemcomm

Negishi coupling reactions with [^{11}C]CH_3I: a versatile method for efficient ^{11}C–C bond formation†

Luka Rejc,*[a] Vanessa Gómez-Vallejo,[a] Jesús Alcázar,[b] Nerea Alonso,[b] José Ignacio Andrés,[b] Ana Arrieta,[c] Fernando P. Cossío[c] and Jordi Llop*[a]

Herein, we present a fast, efficient and general one-pot method for the synthesis of ^{11}C-labelled compounds *via* the Negishi cross-coupling reaction. Our approach, based on the *in situ* formation of [^{11}C]CH_3ZnI and subsequent reaction with aryl halides or triflates, has proven efficient to synthesize [^{11}C]thymidine, a biologically relevant compound with potential applications as a proliferation marker. Theoretical calculations have shown irreversible formation of a tetracoordinated nucleophilic ^{11}C–Zn(II) reagent and electronic requirements for an efficient Negishi coupling.

Emerging applications in positron emission tomography (PET)[1] have resulted in a boost in the demand for new positron-emitter-labelled radiotracers. Carbon-11 (^{11}C; $t_{1/2}$ = 20.4 min) is one of the most attractive positron emitters because its stable isotopes form the main building blocks of all organic molecules, providing an opportunity to prepare a wide variety of radiolabelled organic compounds through ^{11}C-methylation, ^{11}C-cyanation, ^{11}C-carbonylation, and ^{11}C-carboxylation.[2] Among these, the most frequently used method is ^{11}C-methylation, which encompasses a fast and efficient S_N2 nucleophilic substitution reaction using the easily produced labelling agent [^{11}C]CH_3I.[3] However, it is limited to the production of [^{11}C]methoxides, [^{11}C]methylamines, and [^{11}C]methylthio compounds. Recently reported possibilities for radiolabelling *via* palladium(0)-mediated cross-coupling reactions to form ^{11}C–C bonds (Scheme 1a) do not offer a general alternative.[4] The direct ^{11}C–C coupling between [^{11}C]CH_3I and aryl stannanes or aryl boronic acids indeed results in [^{11}C]methylaryl-based compounds; however, the preparation, isolation, and purification of the required precursors is sometimes challenging or even impossible.[5] Additionally, the Stille reaction has been found to result in low molar radioactivity (MA) and is hampered by the biotoxicity of organotin reagents.[6] The use of [^{11}C]methyl-tin and [^{11}C]methyl-lithium reagents enabled [^{11}C]methylation reactions on more accessible substrates, but the formation and manipulation of the organo-tin and organo-lithium compounds remains challenging.[7] Furthermore, strong polarisability of the C–Li bond makes methyllithium highly nucleophilic, diminishing its selectivity and group tolerance.

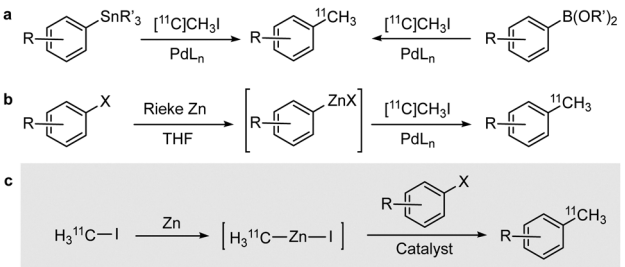

Scheme 1 (a) [^{11}C]methyl-arene synthesis *via* Stille (left) or Suzuki (right) [^{11}C]methylation reactions; (b) two-step radiolabelling of aryl halides *via* the formation of arylzinc halide and subsequent Negishi reaction with [^{11}C]methyl iodide; (c) two-step one-pot reaction for [^{11}C]methyl-arene synthesis *via* Negishi cross-coupling using *in situ* generated $^{11}CH_3ZnI$, proposed in this study.

Highly specific and versatile Negishi cross-coupling reaction offers an alternative to ^{11}C–C bond formation, as reported recently (Scheme 1b).[8] However, the main challenge remains the preparation of a general [^{11}C]methylating reagent that would omit the preparation of aryl zincates on a case-by-case basis. Within our tracer development program, we devised a unique way to explore the unprecedented reaction of zinc with [^{11}C]CH_3I to form the corresponding umpolung species $^{11}CH_3ZnI$, which might enable direct [^{11}C]methylation of aryl halides (Scheme 1c). The fact that radiochemical reactions proceed under pseudo-first order kinetics in the presence of a

[a] *Radiochemistry and Nuclear Imaging, CIC biomaGUNE, Paseo Miramón 182, 20014 San Sebastián, Guipúzcoa, Spain. E-mail: jllop@cicbiomagune.es, lrejc@cicbiomagune.es; Tel: +34 943 00 53 33*
[b] *Lead Discovery Chemistry–Discovery Sciences, Janssen Research & Development, Jarama 75A, 45007 Toledo, Spain*
[c] *Department of Organic Chemistry I, ORFEO-CINQA, Universidad del País Vasco/Euskal Herriko Unibertsitatea UPV/EHU, Donostia International Physics Center (DIPC), Paseo Manuel Lardizabal 3, 20018 San Sebastián/Donostia, Spain*

† Electronic supplementary information (ESI) available: Detailed experimental details, characterization of new compounds, and computational data. See DOI: 10.1039/c8cc01540f

clear deficiency of the labelling agent led us to hypothesise that the reaction would proceed fast and efficiently.

Hoping to avoid notoriously long procedures of alkyl zincate formation[9] that would impact the final radiochemical yield, we envisaged *in situ* [^{11}C]CH_3ZnI formation in a zinc-filled cartridge, followed by cross-coupling with an aryl halide.[10] At the initial stage, the [^{11}C]methylation of 4-bromoacetophenone to produce 4-[^{11}C]methylacetophenone was explored as a model reaction. Due to high susceptibility of zinc to oxidation, the metal surface was activated with an iodine solution. Iodine rather than the traditionally used trimethylsilyl chloride was selected because of its compatibility with the subsequent cross-coupling reaction and the ability to form higher-order zincate complexes, which reportedly favoured the C–C bond formation.[11] *N*,*N*-Dimethylacetamide (DMA) has been used as a solvent as it promotes the formation/improves the stability of the methyl zincate complex and supports the transition metal-catalyzed cross-coupling reaction. Upon activation, [^{11}C]CH_3I was directly distilled into the cartridge. Promisingly, almost quantitative trapping of [^{11}C]CH_3I in the cartridge (>95%) could be achieved. After 1-minute reaction at 65 °C, the contents were eluted with anhydrous DMA into a vial pre-loaded with tetrakis(triphenylphosphine)palladium(0) ($Pd(PPh_3)_4$) and an aryl halide (see ESI,† Fig. S1a). The reaction was carried out for 15 min at T = 65 °C, and the crude product was analyzed by high performance liquid chromatography equipped with a radioactivity detector (radio-HPLC). A radioactive peak with a retention time (rt) of 6.2 min co-eluted with 4-methylacetophenone in the UV chromatogram. The radiochemical conversion, calculated as the ratio between the area under the peak at rt = 6.2 min and the sum of the areas of all peaks in the chromatogram (radioactive detector), was close to 1%. Interestingly, the highest peak in the chromatogram corresponded to [^{11}C]CH_3I (rt = 4.8 min), suggesting that the reason for the low reaction yield was the lack of formation of the activated species [^{11}C]CH_3ZnI.

Based on a recent theoretical study on the beneficial effects of Pd–Zn bond formation in oxidative addition, transmetalation, and reductive elimination in the Negishi coupling reaction,[12] the introduction of the palladium complex during [^{11}C]methyl-zincate formation was taken into consideration. Indeed, when $Pd(PPh_3)_4$ (10 μmol) was added to the zinc-activating iodine solution, the chromatographic yield increased to 6% (Fig. S1b, ESI†).

To facilitate automatisation and further increase the reaction yield, a one-pot set up was finally designed (Fig. S1c, ESI†). Herein, [^{11}C]CH_3I gas was directly distilled into a zinc-filled cartridge, pre-loaded with a solution containing iodine, 4-bromoacetophenone, and $Pd(PPh_3)_4$ in anhydrous DMA, and the contents of the cartridge were eluted with anhydrous THF after 5 minutes. Moreover, two major radioactive peaks were observed in the chromatogram: the ^{11}C-methylated product, which accounted for 83% of the total radioactivity (Table 1, entry 1) and a peak with an rt = 3.2 min identified as [^{11}C]CH_4, resulting from the immediate and quantitative hydrolysis of [^{11}C]CH_3ZnI in the water-containing chromatographic mobile phase. To confirm the origin of [^{11}C]CH_4, the reaction mixture was analyzed at 1 and 3 minutes. The relative concentration of the radioactive species [^{11}C]CH_4, [^{11}C]CH_3I, and

Table 1 Conversion values (average values, n = 3) obtained for different aryl halides and triflates (T = 60 °C)

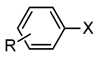
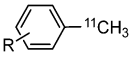

Entry	R	X	Product[a] (%)
1	4-Acetyl	Br	83[b]
2	3-Acetyl	Br	22[b]/35[c]
3	2-Acetyl	Br	30[b]/53[c]
4	4-Ethyl ester	Br	69[b]
5	1-Naphtyl	Br	21[b]
6	4-Amino	Br	19[b]
7	2-Amino	Br	2[b]
8	4-Methoxy	Br	8[b]
9	2,4-Dichloro	I	60 (32)[d]
10	2-Acetyl	I	28 (21)[b,d]
11	1-Naphtyl	I	26 (41)[d]
12	2-Amino	I	12 (28)[d]
13	4-Methoxy	I	33 (22)[d]
14	4-Acetyl	OTf	73[b]
15	4-Methoxy	OTf	0[b]

[a] Calculated as the ratio between the area of the peak corresponding to [^{11}C]methylaryl and the sum of the areas of all the peaks in the radiochromatogram. [b] Reaction time = 5 min. [c] Reaction time of 10 min. [d] In brackets, the amount of [^{11}C]CH_3I left in the solution after reaction.

4-[^{11}C]methylacetophenone followed the expected trend with reaction time: the relative amount of [^{11}C]CH_3I progressively decreased, whereas the ^{11}C-methylated product followed an opposite trend (see ESI,† Fig. S2). The peak corresponding to [^{11}C]CH_4 slightly increased from 1 to 3 minutes, and almost disappeared at 5 minutes, completely disproving the theory of formation of [^{11}C]CH_4 during the reaction and confirming the formation of the active [^{11}C]methyl-zincate complex. Importantly, the [^{11}C]CH_3I trapping was not compromised under these experimental conditions. The possibility of formation of aryl zincate, a possible by-product during the reaction, acting as a nucleophile in the Negishi reaction was rejected by a reverse activation experiment (Fig. S1d, ESI†). In this case, a zinc cartridge was preloaded with a solution of 4-bromoacetophenone and palladium catalyst, and the contents eluted to [^{11}C]CH_3I and $Pd(PPh_3)_4$-filled vial after 5 minutes at 65 °C. No product was observed in the reaction mixture.

To prove the generality of our method and the tolerability to a variety of functional groups, we successfully formed ^{11}C-labelled methyl aryls using different aryl bromides (Table 1, entries 1–8), iodides (entries 9–13), and triflates (entries 14 and 15). In general, electron-withdrawing groups (EWG) (Table 1, entries 1–4) promoted reaction yields, whereas electron-donating group (EDG)-bearing substrates exhibited low conversion values (Table 1, entries 6–8). In all the cases (entries 1–8), the relative amount of [^{11}C]CH_3I remaining in the reaction crude accounted for less than 5% of the total radioactivity. These results, together with the increasing conversion values at longer reaction times (Table 1, entries 2 and 3), further support the kinetic dependency of the reaction on the ability of a substrate-palladium complex formation/dissociation, rather than inactivation of zinc or deactivation of the palladium catalyst.

Surprisingly, parallel reactions with aryl iodides resulted in equivalent or only slightly increased chromatographic yields. Note that in these cases, the presence of a significant amount of

unreacted [^{11}C]CH_3I was detected (in brackets in the table); this suggested hampered formation of the activated ^{11}C-methyl zincate species. Further inspection of the UV chromatograms revealed the presence of additional peaks, identified by GC-MS as the de-iodinated precursor (see ESI,† Fig. S3). De-halogenation, although seen in some aryl bromides, had a bigger effect on aryl iodides, which readily de-halogenated in an activated zinc cartridge at 65 °C after 10 min probably *via* the formation of an arylzinc iodide complex. Similar to the detection of [^{11}C]CH_3ZnI, the formation of arylzincates was only indirectly confirmed by the detection of a de-halogenated product after hydrolysis. De-halogenation yields followed the trend observed for the oxidative addition to palladium; thus, higher de-halogenation was observed for EWG-bearing aryl iodides.

To better understand the origins of our results, we performed DFT calculations at the B3LYP(SCRF)-D3/6-31G(d)&LANL2DZ[13] theoretical level. Both experimental and theoretical studies[14] indicate that in the presence of coordinating solvents such as THF, solvated Zn(II)-containing species are the nucleophiles present in the Negishi coupling. In effect, our calculations show that when DMA is used as a solvent, the reaction of [^{11}C]CH_3I with solvated zinc yields the tetracoordinated species **1** *via* a highly exergonic process (Fig. 1a). The nucleophilic intermediate **1** shows a tetrahedral coordination pattern, as expected for a d^{10} Zn(II) metallic centre, and enters into the catalytic cycle shown in Fig. 1b.[12,15]

According to this mechanism, the catalyst $Pd(PPh_3)_2$ reacts with the alkyl halide **2** to give rise to adduct **3**. This intermediate reacts with **1** to yield the isomeric products **5** *via* a quite complex process in which heterobimetallic intermediates are involved. Many previous experimental and computational mechanistic studies[16] have focused on these stages of the catalytic cycle. Formation of both ***cis*-5** and ***trans*-5** is a quite fast process, the latter being even faster. However, ***cis*-5** intermediates are thermodynamically more stable than their *trans* congeners. For instance, in our case, ***cis*-5b** (R = 2-NH_2, see Fig. 2) is calculated to be 4.1 kcal mol^{-1} more stable than ***trans*-5b**. The ^{11}C–C bond forming step is slower and determines the reaction rate. This reductive elimination step yields adduct **6** *via* the saddle point **TS**, with concomitant release of the catalyst $Pd(PPh_3)_2$ and completion of the catalytic cycle (Fig. 1b).

The energy profile associated with the ***cis*-5** → **6** + $Pd(PPh_3)_2$ transformation was then computed. We selected three substitution patterns **a**, **b**, and **c**, in which the electrophilicity of the aryl moiety varied according to the electron-withdrawing or electron-releasing character of the R substituent. In the three cases, we located three-membered cyclic transition structures **TSa–c** (Fig. 2) that were quite synchronous. When we computed the reaction profiles associated with the ***cis*-5a** → **6a** + $Pd(PPh_3)_2$ process for ^{12}C and ^{13}C isotopes at the methyl moiety arising from MeI, we obtained very similar relative Gibbs energies for the [^{11}C]Me and [^{12}C]Me groups. However, a noticeable increase in the activation free energy was computed while transitioning from [^{11}C]Me to [^{13}C]Me, with $\Delta\Delta G^{\ddagger}_{333} = \Delta G^{\ddagger}_{333}(^{13}C) - \Delta G^{\ddagger}_{333}(^{11}C) = +0.3$ kcal mol^{-1}, which corresponded to an estimated KIE of *ca.* 1.6. We found that the computed free activation energies at

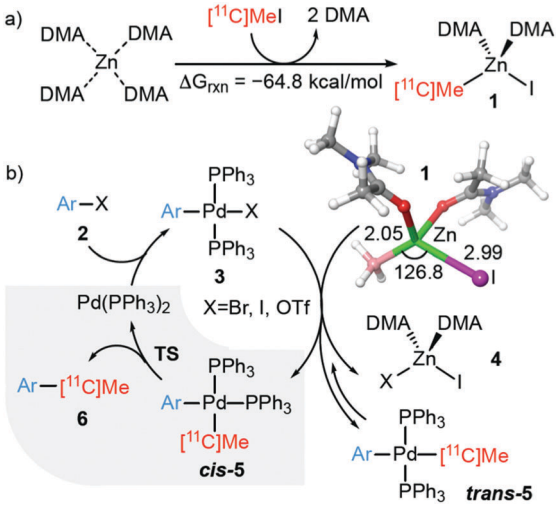

Fig. 1 (a) The calculated free reaction energy (B3LYP-D3(SCRF=DMA)/6-31G(d)&LANL2DZ level of theory T = 333.15 K) associated with the formation of nucleophile **1** from solvated $Zn^0\cdots(DMA)_4$ and [^{11}C]CH_3I. (b) Chief geometric features of tetrahedral species **1** and catalytic cycle associated with the formation of adducts **6**. The rate-determining step leading to the reaction product *via* transition structure **TS** is highlighted in grey and presented in more detail in Fig. 2. DMA: *N,N*-dimethylacetamide. Bond distances and ^{11}C–Zn–I bond angle are given in Å and deg., respectively.

333.15 K correlated with the electrophilicity of the reactants ***cis*-5a–c** estimated by means of the electrophilic local Fukui functions f^{+}[17] calculated at the carbon atom of the aryl moiety involved in the formation of the C_x–^{11}C bond (Fig. 2). In the case of the formation of the adduct **6a**, in which R = 4-Ac, the f^{+} value is highest, and the associated Gibbs activation energy was found to be lowest. This is in good agreement with the high yield obtained for this reaction (Table 1, entry 1). When we analyzed the reactivity of the adducts ***cis*-5b and c**, where R = 2-NH_2 and R = 4-OMe, respectively (Fig. 2), we found that the local electrophilicities were negligible, and the activation energies were 2.0–2.7 kcal mol^{-1} higher than that calculated for **TSa**. These higher values and the corresponding lower reaction rates are in line with the low yields found in the Negishi couplings between [^{11}C]CH_3I and 2-bromoaniline (Table 1, entry 7) and 1-bromo-4-methoxybenzene (Table 1, entry 8). Moreover, in these latter two cases, the complexes **6b′** and **6c′** were found, in which the coupling products **6b** and **c** were bound to the catalyst by means of a weak hydrogen bond and a Wheland-like interaction, respectively. Therefore, we conclude that in the cases involving electron-rich coupling products, release of the catalyst and completion of the catalytic cycle can be partially hampered by weak inhibition of the catalyst by the adduct generated after the reductive elimination step.

As a proof of the suitability of our method to prepare biologically relevant compounds, we tackled the synthesis of [^{11}C]thymidine (proliferation marker), starting from 5-iodo-2′-deoxyuridine (Scheme 2). The synthesis resulted in a 53% radiochemical conversion in the 5 min reaction. Inclusion of a purification step (see ESI†) resulted in pure [^{11}C]thymidine with a 6.1% radiochemical yield and MA > 50 GBq μmol^{-1}.

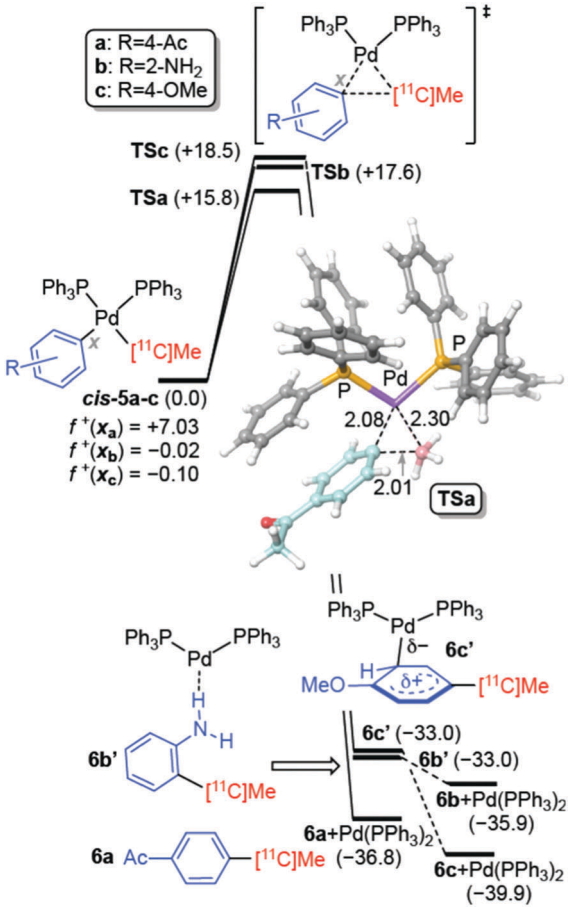

Fig. 2 Calculated reaction profiles (B3LYP-D3/6-31G*&LANL2DZ level of theory) of the C–C bond forming step of Negishi reactions involving [^{11}C]-complexes **1a–c**. Numbers in parentheses are relative Gibbs energies calculated at 333.15 K. Bond distances and energies are given in Å and kcal mol^{-1}, respectively. Local values of the electrophilic Fukui function f^+ on atoms C*x* are given in a.u. × 10^3.

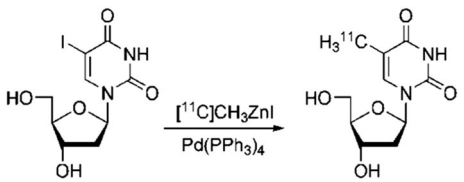

Scheme 2 Formation of [^{11}C]thymidine from the commercially available 5-iodo-2′-deoxyuridine.

Our study confirms that the Negishi cross-coupling reaction of *in situ* formed [^{11}C]MeZnI can be performed with aryl halides and triflates commonly available in medicinal chemistry programs. Good yields and high group tolerability should enable the preparation of a wide range of ^{11}C-labelled biologically relevant compounds, as demonstrated with the synthesis of [^{11}C]thymidine. Together with the development of new metal complexes, our simple and general method provides a new alternative of ^{11}C-radiolabelling and may change the way of how ^{11}C-radiochemistry can be carried out in the future. Further applications of this approach will be matters of future research.

Financial support for this work was provided by the Spanish MINECO (CTQ2017-87637-R, CTQ2016-80375-P and CTQ2016-81797-REDC) and Eusko Jaurlaritza (GV/EJ, Grant IT673-13).

Conflicts of interest

The authors declare no conflict of interest.

Notes and references

1 J. S. Fowler and N. D. Volkow, *Neuroscience in the 21st Century: From Basic to Clinical*, 2nd edn, 2016, pp. 2929–2954.
2 (*a*) P. W. Miller, N. J. Long, R. Vilar and A. D. Gee, *Angew. Chem., Int. Ed.*, 2008, **47**, 8998; (*b*) O. Itsenko, V. Goméz-Vallejo, J. Llop and J. Koziorowski, *Curr. Org. Chem.*, 2013, **17**, 2067.
3 R. Bolton, *J. Labelled Compd. Radiopharm.*, 2001, **44**, 701.
4 K. Dahl, C. Halldin and M. Schou, *Clin. Transl. Imaging*, 2017, **5**, 275.
5 T. Hosoya, K. Sumi, H. Doi, M. Wakao and M. Suzuki, *Org. Biomol. Chem.*, 2006, **4**, 410.
6 (*a*) J. Madsen, P. Merachtsaki, P. Davoodpour, M. Bergström, B. Långström, K. Andersen, C. Thomsen, L. Martiny and G. M. Knudsen, *Bioorg. Med. Chem.*, 2003, **11**, 3447; (*b*) L. Samuelsson and B. Långström, *J. Labelled Compd. Radiopharm.*, 2003, **46**, 263; (*c*) M. Huiban, S. Pampols-Maso and J. Passchier, *Appl. Radiat. Isot.*, 2011, **69**, 1390.
7 (*a*) M. Huiban, A. Huet, L. Barré, F. Sobrio, E. Fouquet and C. Perrio, *Chem. Commun.*, 2006, 97; (*b*) D. Heijnen, F. Tosi, C. Vila, M. C. A. Stuart, P. H. Elsinga, W. Szymanski and B. L. Feringa, *Angew. Chem., Int. Ed.*, 2017, **56**, 3354.
8 S. Kealey, J. Passchier and M. Huiban, *Chem. Commun.*, 2013, **49**, 11326.
9 S. Huo, *Org. Lett.*, 2003, **5**, 423.
10 (*a*) L. Huck, M. Berton, A. De La Hoz, A. Díaz-Ortiz and J. Alcázar, *Green Chem.*, 2017, **19**, 1420; (*b*) N. Alonso, L. Z. Miller, J. De, M. Muñoz, J. Alcázar and D. T. McQuade, *Adv. Synth. Catal.*, 2014, **356**, 3737; (*c*) M. Berton, L. Huck and J. Alcázar, *Nat. Protoc.*, 2018, **13**, 324.
11 L. C. McCann, H. N. Hunter, J. A. C. Clyburne and M. G. Organ, *Angew. Chem., Int. Ed.*, 2012, **51**, 7024.
12 B. Fuentes, M. García-Melchor, A. Lledós, F. Maseras, J. A. Casares, G. Ujaque and P. Espinet, *Chem. – Eur. J.*, 2010, **16**, 8596.
13 (*a*) C. Lee, W. Yang and R. G. Parr, *Phys. Rev. B: Condens. Matter Mater. Phys.*, 1988, **37**, 785; (*b*) A. D. Becke, *J. Chem. Phys.*, 1993, **98**, 1372; (*c*) A. D. Becke, *J. Chem. Phys.*, 1993, **98**, 5648; (*d*) J. Tomasi, B. Mennucci and R. Cammi, *Chem. Rev.*, 2005, **105**, 2999; (*e*) M. J. Frisch *et al.*, *Gaussian 09, Revision B.01*, Gaussian, Inc., Wallingford CT, 2009, see ESI† for the full reference.
14 J. Del Pozo, M. Pérez-Iglesias, R. Álvarez, A. Lledós, J. A. Casares and P. Espinet, *ACS Catal.*, 2017, **7**, 3575.
15 M. García-Melchor, A. A. C. Braga, A. Lledós, G. Ujaque and F. Maseras, *Acc. Chem. Res.*, 2013, **46**, 2626.
16 (*a*) M. García-Melchor, B. Fuentes, A. Lledós, J. A. Casares, G. Ujaque and P. Espinet, *J. Am. Chem. Soc.*, 2011, **133**, 13519; (*b*) Q. Liu, Y. Lan, J. Liu, G. Li, Y. D. Wu and A. Lei, *J. Am. Chem. Soc.*, 2009, **131**, 10201.
17 P. W. Ayers, W. Yang and L. J. Bartolotti, in *Chemical Reactivity Theory: A Density Functional TheoryView*, ed. P. Chattaraj, Taylor & Francis, Boca Raton, 2009, pp. 255–267.